Materials Research Letters
Publication details, including instructions for authors and subscription information:
http://www.tandfonline.com/loi/tmrl20

A Critical Review of the Oxidation of Ti_2AlC, Ti_3AlC_2 and Cr_2AlC in Air

Darin J. Tallman [a], Babak Anasori [a] & Michel W. Barsoum [a]
[a] Materials Science and Technology, Drexel University, Philadelphia, PA, 19104, USA
Published online: 08 Jun 2013.

To cite this article: Darin J. Tallman, Babak Anasori & Michel W. Barsoum (2013) A Critical Review of the Oxidation of Ti_2AlC, Ti_3AlC_2 and Cr_2AlC in Air, Materials Research Letters, 1:3, 115-125, DOI: 10.1080/21663831.2013.806364

To link to this article: http://dx.doi.org/10.1080/21663831.2013.806364

MATERIALS RESEARCH LETTERS

Mater. Res. Lett., 2013
Vol. 1, No. 3, 115–125, http://dx.doi.org/10.1080/21663831.2013.806364

Taylor & Francis
Taylor & Francis Group

www.tandfonline.com/toc/tmrl000/current

A Critical Review of the Oxidation of Ti_2AlC, Ti_3AlC_2 and Cr_2AlC in Air

Darin J. Tallman*, Babak Anasori and Michel W. Barsoum

Materials Science and Technology, Drexel University, Philadelphia, PA 19104, USA

(*Received 20 February 2013; final form 13 May 2013*)

Of all the $M_{n+1}AX_n$ phases, the most resistant to oxidation in air in the 900–1,400°C temperature range are Ti_2AlC, Ti_3AlC_2 and Cr_2AlC. A literature review, however, shows that while many claim the oxidation kinetics to be parabolic, others claim them to be cubic. Whether the kinetics are parabolic or better is of vital practical importance. By carefully re-plotting the results of others and carrying out one oxidation run for ≈3,000 h at 1,200°C on a Ti_2AlC sample, we conclude that the oxidation kinetics are better described by cubic kinetics and that even that conclusion is an approximation. Lastly, we present compelling evidence that the rate-limiting step during the oxidation of Ti_2AlC is diffusion down the alumina scale grain boundaries.

Keywords: Ti_2AlC, Cr_2AlC, Ti_3AlC_2, Oxidation, Cubic Oxidation Rate

Introduction The $M_{n+1}AX_n$ (MAX) phases are a class of layered, machinable, early transition ternary metal carbides and/or nitrides, where M is an early transition metal, A is a group 13–16 element, and X is C and/or N. These compounds are classified as thermodynamically stable nanolaminates having relatively high fracture toughness values (8–12 MPa$\sqrt{m}$), and yet are machinable, lightweight and relatively soft.[1–5] Some also undergo a brittle-to-plastic transition at temperatures above 1,000°C. Some aluminum, Al, containing MAX phases, notably Ti_3AlC_2, Ti_2AlC and Cr_2AlC show excellent oxidation resistance due to the formation of a dense and adherent alumina layer. These ternary carbides may prove useful in practical applications where high-temperature oxidation resistance in air is required. However, before they can be used it is imperative to be able to predict the oxide thicknesses that would form after long times at elevated temperatures. This is in turn implies that the oxidation kinetics be well understood and documented.

Literature Survey The first papers to report on the oxidation of the $Ti_{n+1}AlX_n$ phases were published in 2001.[6,7] In these papers, it was shown that the oxidation resulted in the formation of a rutile-based solid solution with approximate chemistry of $(Ti_{1-y}Al_y)O_{2-y/2}$, where $y \approx 0.05$ and alumina, Al_2O_3 (Figure 1(a)). At longer times, kinetic demixing resulted in the formation of layers of rutile henceforth referred to as TiO_2, Al_2O_3 and porous layers (Figure 1(b)).

The oxidation kinetics were initially found to be parabolic, but at longer times tended towards linear, implying that the layers were not protective over the long run. Using Wagner's formalism it was further concluded that the rate-limiting step was the inward diffusion of oxygen and the outward diffusion of titanium through the TiO_2 layer that forms. In other words, the oxidation reaction was presumed to be [6]

$$2Ti_2AlC + 7.5O_2 = 4TiO_2 + Al_2O_3 + 2CO_2. \quad (1)$$

The C was presumed to diffuse through the rutile layer and oxidize. As discussed below, when the oxide that forms is TiO_2, the oxidation resistance is poor. Fortuitously, in many cases, the oxide that forms is Al_2O_3, in which case the oxidation resistance is excellent. In the remainder of this paper, the discussion will deal exclusively with oxidation that results in the formation of dense protective Al_2O_3 layers.

Ti_2AlC. Following the initial work in 2001, there have been many studies that have explored the oxidation behavior of Ti_2AlC. In 2003, Wang and Zhou quantified the oxidation kinetics of Ti_2AlC as cubic by heating it in

*Corresponding author: Emails: tallman@drexel.edu, darintallman@gmail.com

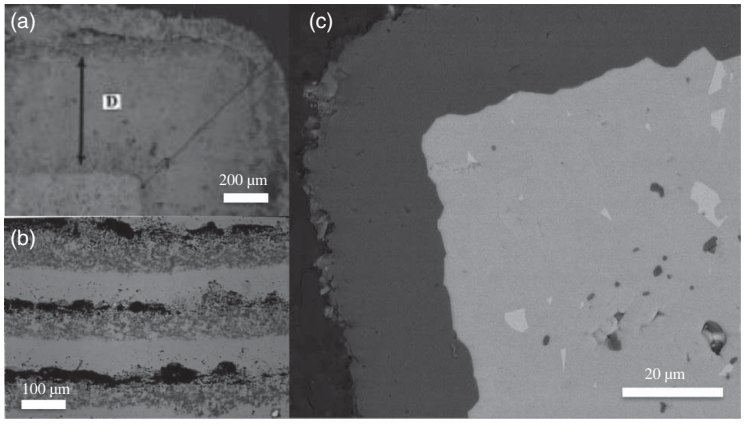

Figure 1. (a) Oxidation of the $Ti_{n+1}AlX_n$ phases results in the formation of a rutile-based solid solution with approximate chemistry of $(Ti_{1-y}Al_y)O_{2-y/2}$, where $y \approx 0.05$ and alumina, Al_2O_3. (b) At longer times, kinetic demixing results in the formation of layers of TiO_2, Al_2O_3 and pores.[6] (c) Scanning electron microscope, SEM, micrograph of Ti_2AlC oxidized in air at 1,200°C for 2,873 h showing $a \approx 21$ μm thick, coherent and fully dense Al_2O_3 layer which conforms to the corners of the sample.

air for 20 h in the 1,000–1,300°C temperature range.[8] In other words, they concluded that the oxidation kinetics were best described by

$$\left(\frac{\Delta w}{A}\right)^3 = k_c t, \tag{2}$$

where Δw is the weight gain, A is the surface area exposed to the atmosphere, t is the time and k_c is the cubic reaction rate constant. In this case, the overall simplified reaction is assumed to be

$$Ti_2AlC + \left(\frac{3x}{4} + y\right) O_2 = \left(\frac{x}{2}\right) Al_2O_3 + Ti_2Al_{1-x}C_{1-y} + yCO_2 \quad x < 0.5. \tag{3}$$

Here again, the C is presumed to diffuse through the Al_2O_3 layer and oxidize. A typical microstructure of a Ti_2AlC sample oxidized for almost 3,000 h at 1,200°C is shown in Figure 1(c). Note that the reaction layer comprises almost pure Al_2O_3 and that it conforms to the samples' corners.

In 2004, Sundberg et al. reported parabolic oxidation kinetics for Ti_2AlC up to 1,400°C in air.[9] In 2007, Byeon et al. reported that the oxidation kinetics were *cubic* in isothermal and cyclical oxidation tests at 1,000°C, 1,200°C and 1,400°C.[10] Contrary to their previously published work in which it was claimed that the kinetics were cubic,[8] in a recent review article, Wang and Zhou reported that Ti_2AlC exhibited parabolic behavior.[11] In 2011, Cui et al. reported parabolic kinetics for Ti_2AlC up to 1,400°C.[12] In 2012, Yang et al. reported cubic kinetics for Ti_2AlC at 1,200°C.[13] Basu et al. also reported cubic oxidation kinetics for Ti_2AlC in both air and steam in the 1,000–1,300°C temperature range.[14]

Ti_3AlC_2. The oxidation behavior of Ti_3AlC_2 has been less widely studied. In 2003, Wang and Zhou reported that the kinetics were parabolic.[15] Qian et al. reported the oxidation kinetic to be parabolic, in the 1,000–1,300°C range.[16] Lee and Park [17] reported that the oxidation kinetics were temperamental; some samples formed predominantly TiO_2 layers, others formed Al_2O_3 layers in which case the oxidation reaction is presumably

$$Ti_3AlC_2 + \left(\frac{3x}{4} + y\right) O_2 = \left(\frac{x}{2}\right) Al_2O_3 + Ti_3Al_{1-x}C_{2-y} + yCO_2, \quad x < 0.5. \tag{4}$$

Needless to add, the samples that formed an Al_2O_3 layer were quite oxidation resistant. As noted above, when the oxide layers formed were TiO_2-based, the resulting oxidation resistance was poor.

Cr_2AlC. In 2007, Lin et al. reported that the oxidation kinetics for Cr_2AlC in the 800–1,300°C range were parabolic.[18] The overall oxidation reaction was surmised to be

$$28\,Cr_2AlC + 25\,O_2 = 14\,Al_2O_3 + 8\,Cr_7C_3 + 4\,CO_2. \tag{5}$$

In this case, a continuous Cr_7C_3 sub-layer formed between the protective alumina layer and the Cr_2AlC substrate (Figure 2). As discussed below, the presence of this sub-layer has important implications and ramifications.

At 1,300°C, the Al_2O_3 layer has a tendency to spall off and the oxidation resistance is compromised.[19] In 2008, Lee et al. further showed that the cyclic oxidation resistance of Cr_2AlC in air to be excellent at 1,000°C, good at 1,100°C, intermediate at 1,200°C, but poor at 1,300°C.[20] Hajas et al., in 2011, reported parabolic oxidation kinetics for Cr_2AlC thin films in the 1,230–1,410°C range.[21] Most recently, in 2012, Li et al. explored the effect of grain size on oxidation kinetics of Cr_2AlC: coarse-grained (CG) samples exhibited cubic

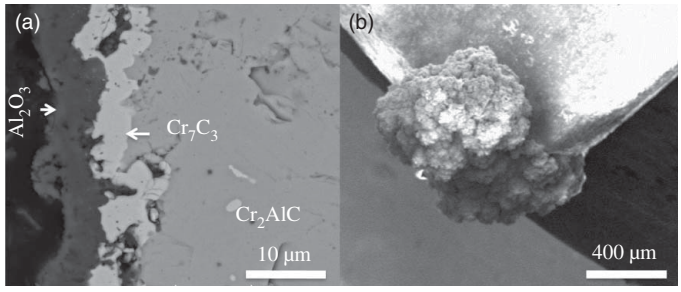

Figure 2. SEM micrograph of (a) cross-sectioned Cr_2AlC sample oxidized at 1,200°C. The outer layer is a Cr-containing Al_2O_3 and the inner layer is Cr_7C_3; (b) of sample oxidized at 1,100°C for 35 h clearly showing Cr_2O_3 nodules (Gupta, unpublished results). This is the only MAX phase to show the formation of a carbide layer beneath the oxide layers formed during oxidation.

oxidation kinetics at 1,100 and 1,200°C, whereas fine-grained (FG) samples were less than parabolic at 1,100°C and cubic at 1,200°C.[22] Also in 2012, Lee et al. showed that at 1,200°C, after a period of about 10 h during which there was an increase in weight, beyond that time the samples lost weight more or less linearly.[23]

Parabolic, Cubic or Power Law Kinetics The brief review of the literature of the oxidation of Ti_2AlC, Ti_3AlC_2 and Cr_2AlC makes it amply clear that most agree on one fact, namely the formation of an alumina layer is critical, endowing these compounds with their excellent oxidation resistance. When rutile forms instead, the oxidation resistance is greatly diminished. Where there is quite a bit of disagreement, however, is whether the kinetics are cubic or parabolic. This distinction is of outmost importance, because if the kinetics are indeed parabolic, then the long-term prognosis is *not* good. However, if the kinetics are slower than parabolic, e.g. cubic or even better, then the oxidation resistance would be good enough for practical applications. This is a crucial point that needs to be established beyond a reasonable doubt since many, following the lead of Wang and Zhou, also assumed parabolic oxidation kinetics. The same conclusion was reached in a recent review article [11] despite the fact that Byeon et al. [10] and more recently Basu et al. [14] clearly showed the kinetics to be cubic. More problematic is that most of the studies on the oxidation of Cr_2AlC to date claim parabolic oxidation kinetics, including a recent review article on this compound.[11,18–20,24]

In the remainder of this paper, we emphatically make the case that the oxidation kinetics are better described as cubic, and quite comparable for the three compounds. The latter conclusion should not be surprising given that a dense, cohesive Al_2O_3-rich layer forms in all cases. We make our case using a two-pronged approach. The first is to re-plot some of the results of the early papers in which the authors maintained that the oxidation kinetics were parabolic and show that they can be better described by cubic kinetics (i.e. Equation (2)). The second is to report on the longest oxidation experiment carried out to date on Ti_2AlC at 1,200°C that clearly show the oxidation kinetics to be cubic or near cubic. Before proceeding further, we note that typically three laws have been used to describe the oxidation kinetics of alumina formation in literature: parabolic, cubic and power law given by, respectively,

$$\Delta x^2 = K' \left(\frac{t}{t_o}\right), \tag{6}$$

$$\Delta x^3 = K' \left(\frac{t}{t_o}\right), \tag{7}$$

$$\Delta x = K' \left(\frac{t}{t_o}\right)^n, \tag{8}$$

where Δx is the oxide scale thickness (μm), $t_o = 1$ s, K' is a constant and n is the power law scale growth exponent. In the following sections, we critically assess which law best fits the oxidation of Ti_3AlC_2, Ti_2AlC and Cr_2AlC.

Ti_2AlC and Ti_3AlC_2. When the results of Wang and Zhou reported in [15] for Ti_3AlC_2 are re-plotted as $(\Delta w/A)^3$ vs. t (Figure 3(a)) least-squares fits of the data resulted in R^2 values that were quite high (>0.998). The R^2 value for the parabolic plot given by the authors (Figure 2 in [15]) is around 0.98. In other words, their own results fit a cubic law better than a parabolic one. It thus makes more sense to assume the kinetics to be cubic.

Also plotted in Figure 3(a) are the results by the same authors reported in [8] for Ti_2AlC. This side-by-side comparison makes it clear that the kinetics for both compounds are not only both cubic, but as importantly, of the same order of magnitude. At 1,100°C, the oxidation kinetics for both ternary phases are nearly identical as they should be if in *both* cases, a dense alumina layer forms. Given the latter, it is highly unlikely that the kinetics would be parabolic in one case (Ti_3AlC_2) and cubic (Ti_2AlC) in the other. This conclusion is further confirmed when the post-oxidation microstructures are compared. After 20 h oxidation at 1,300°C, the Al_2O_3 layer thickness is ≈25 μm in Ti_2AlC and ≈14 μm in Ti_3AlC_2. After 20 h at 1,200°C, the oxide

Figure 2a: Correction

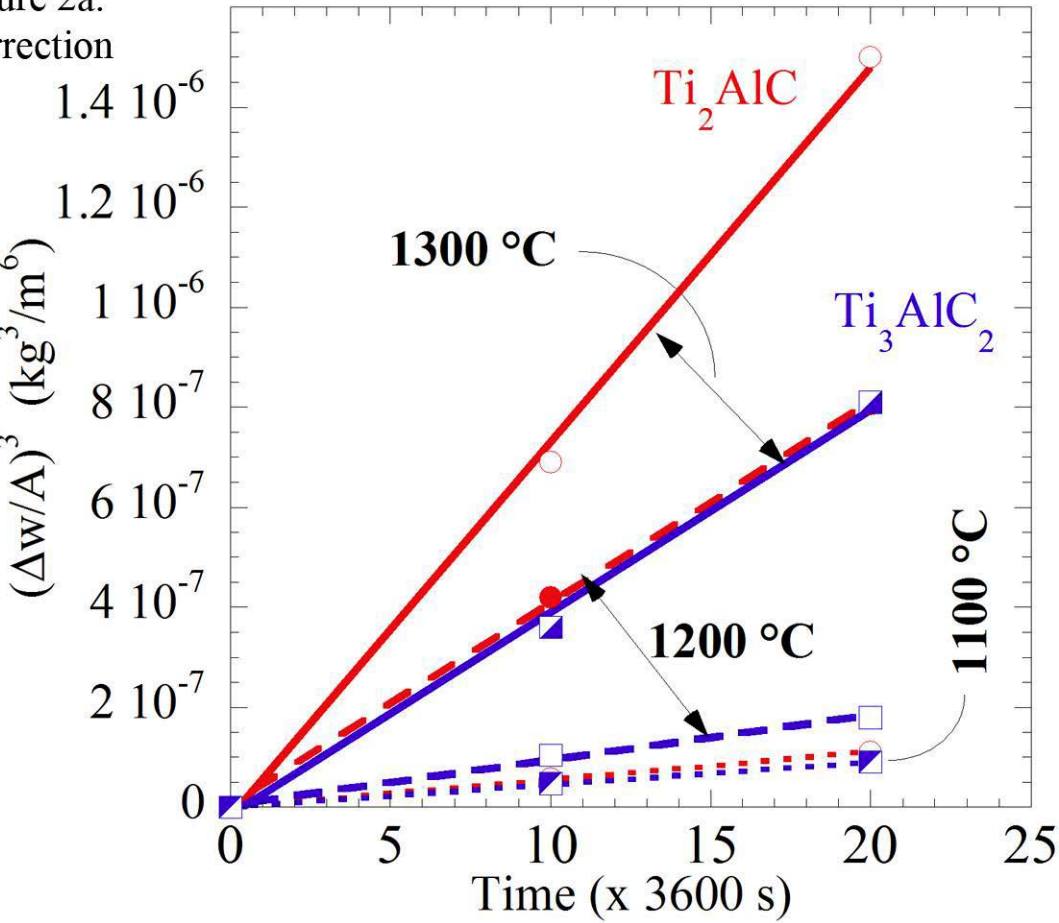

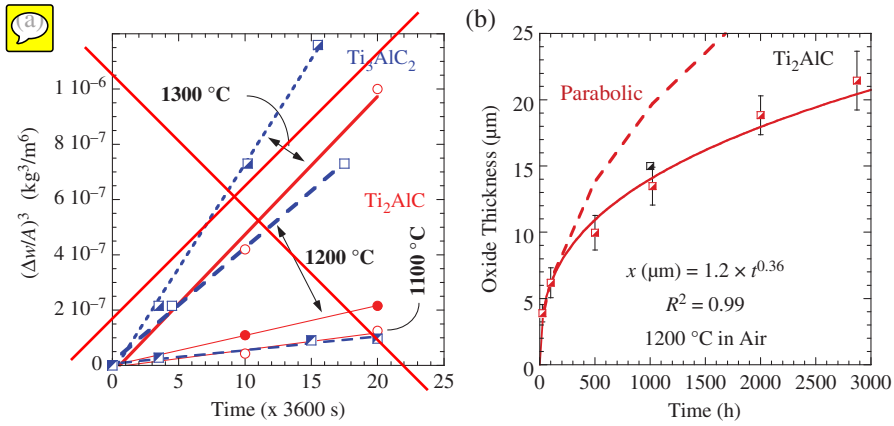

Figure 3. (a) Replotted results from the 2003 Wang and Zhou papers on the oxidation of Ti_3AlC_2 and Ti_2AlC [8,15] showing a linear fit when $(\Delta w/A)^3$ is plotted vs. t. Least-squares fit of the 1,300°C plot results in an R^2 value of 0.998, compared to 0.98 for the parabolic fit reported in the original articles. The compounds and graphs are color coded for clarity. (b) Oxide scale thickness (x) versus time for Ti_2AlC held at 1,200°C for >2,800 h. A power fit of the results shown yields a time exponent of 0.36, viz. cubic kinetics. Dashed line shows the Δx based on a parabolic rate constant fitted to the first 100 h of oxidation. The black square shows Byeon et al. results after 1000, 1 h cycles to 1,200 °C.[10]

layer thicknesses—at ≈5 μm—are almost identical for both compounds.[8,15]

Furthermore, Byeon et al. showed that when commercially available Ti_2AlC polycrystalline samples were heated in air, a continuous, adherent α-Al_2O_3 formed.[10] They also concluded that the oxidation kinetics were cubic.[10] The thickness of the layer was ≈15 μm after 25 h of isothermal oxidation at 1,400°C. Roughly, the same thickness was observed after 1,000 one hour cycles from ambient temperature to 1,200°C. In both cases, the layers remained adherent and protective (Figure 4(a)).

Similarly, recent results by Basu et al. [14] on the oxidation of commercially available Ti_2AlC samples also showed that: (i) the oxidation kinetics up to 120 h were *cubic*; (ii) there is little difference between oxidation in air and in a 100% steam environment up to 1,300°C; (iii) the activation energy was about 270 kJ/mol and (iv) the oxidation results in a continuous and stable layer of α-Al_2O_3, along with a thin surface layer of rutile in both environments. The thin TiO_2 layer, however, volatilizes by forming gaseous $TiO(OH)_2$ in the presence of water vapor at temperatures >1,200°C.

To help resolve this question, we conducted an isothermal oxidation experiment on Ti_2AlC at 1,200°C for >2,800 h. Samples were prepared by pouring pre-reacted Ti_2AlC powders (Kanthal, Sweden) in a graphite die that was in turn placed in a hot press and hot pressed, HPed, for 4 h at 1,300°C under a load corresponding to a stress of ≈30 MPa and a vacuum of 10^{-2} torr. The resulting fully dense samples were electro-discharged machined into smaller blocks ($10 \times 5 \times 3$ mm^3) with a final surface preparation of 1 μm diamond suspension polish.

The initial dimensions and weights were recorded. Samples were then loaded into a box furnace and held at 1,200°C for 25, 100, 500, 1,000, 2,000 and 2,873 h. After almost 3,000 h, the resulting microstructure (Figure 1(c)) clearly shows the formation of a thin cohesive Al_2O_3 layer. After holding at 1,200°C for up to 2,873 h, the oxide layer reached a thickness of about 21 μm (Figure 1(c)). Grain size was measured using the line intercept method on fractured surfaces (Figure 9). About 200 grains per sample were measured.

When Δx^3 is plotted vs. t, a straight line (not shown) is obtained. Least-squares fit of the results resulted in an $R^2 > 0.988$. To further confirm the cubic kinetics, a power law fit (Equation (8)) of the results (Figure 3(b)) resulted in the following relationship:

$$\Delta x(\mu\text{m}) = 1.2\left(\frac{t}{t_o}\right)^{0.36} \qquad R^2 = 0.99, \qquad (9)$$

where $t_o = 1$ s. At 14 μm, the Al_2O_3 layer thickness observed after 1,000 h is in very good agreement to the 15 μm found after 1,000, 1 h cycles to 1,200°C conducted by Byeon et al.,[10] shown in Figure 3(b) as a black square. Based on these results and previous work, it is reasonable to conclude that the oxidation kinetics of Ti_2AlC are indeed near cubic. Table 1 summarizes the k_c values obtained from the various studies on Ti_2AlC, Ti_3AlC_2 and Cr_2AlC.

What is noteworthy and of great practical importance is the fact that even after this extended time at 1,200°C, no cracks were observed anywhere, not even at the corners (Figure 1(c)). One of the main reasons why the oxidation resistance of Ti_2AlC is as good as it is, and so resistant to thermal cycling, is the excellent match in thermal expansions between it and the α-Al_2O_3 protective layer that forms. Photoluminescence of the α-Al_2O_3 scale indicated that the residual stresses formed in that layer were compressive, a function of time and temperature and of the order of 500 MPa (Figure 4(a)).[10] Such residual stresses are considered low, and partially explain the high spallation resistance of the α-Al_2O_3 scale (Figure 4(b)).

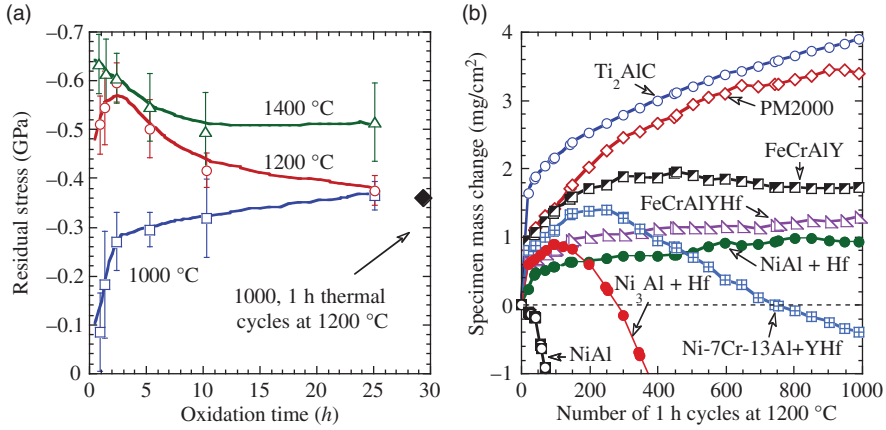

Figure 4. (a) Magnitude of compressive residual stress within the Al_2O_3 scale determined from luminescence-shifts as a function of time of isothermal oxidation at 1,000, 1,200 and 1,400°C.[10] The residual stresses are compressive, a function of time and temperature, and of the order of 500 MPa which is considered low.[10] (b) Oxidation kinetics of Ti_2AlC are compared with other more established/commercial oxidation-resistant alloys. Note that if the very first oxidation cycle is omitted from the Ti_2AlC results, its oxidation kinetics are comparable to PM2000.[10]

Table 1. Summary of k_c ($kg^3m^{-6}s^{-1}$) values for the oxidation of Ti_2AlC, Ti_3AlC_2 and Cr_2AlC.

Phase	1,000°C	1,100°C	1,200°C	1,300°C	1,400°C	Comments and Ref.
Ti_2AlC[a]	~~3.2~~ $\times 10^{-13}$	~~1.1~~ $\times 10^{-12}$	~~3.0 $\times 10^{-12}$~~	~~1.5~~ $\times 10^{-11}$		[8]
Ti_2AlC	3.3×10^{-13}	1.9×10^{-12}	1.0×10^{-11}	5.1×10^{-11}		Air [14]
Ti_2AlC	5.6×10^{-13}	2.0×10^{-12}	1.2×10^{-11}	6.0×10^{-11}		100% H_2O [14]
Ti_3AlC_2		~~1.7~~ $\times 10^{-12b}$	~~3.2~~ $\times 10^{-12b}$	~~2.0~~ $\times 10^{-11b}$	~~6.3~~ $\times 10^{-10b}$	[15]
Cr_2AlC			3.8×10^{-12b}	3.2×10^{-11b}		[18]
Cr_2AlC CG		2.8×10^{-13b}	9.7×10^{-12b}			[22]
Cr_2AlC FG		7.5×10^{-13b}	1.47×10^{-11b}			[22]
Cr_2AlC		4.4×10^{-13b}				[23]

[a]In [8], the results listed in their Table 1 are wrong. The correct values, based on the results they show in their Figure 1(c), are listed here and are the correct ones.
[b]These values are calculated from the weight gain results reported in the original papers. In the original papers, k_c was either not provided or incorrectly reported as parabolic.

Figure 4(b) compares the oxidation kinetics of Ti_2AlC with other more established/commercial oxidation-resistant alloys.[10] We note in passing that commercially available Fe- and Ni-based Al_2O_3-forming alloys have relatively high coefficient of thermal expansions, CTEs, and typically require reactive element additions to improve their spallation resistance.[25] Also note that if the very first oxidation cycle is omitted from the Ti_2AlC results, its oxidation kinetics are comparable to PM2000 (Figure 4(b)).

After heating Ti_2AlC to 1,200°C, and cooling to room temperature, Cui et al. identified twins and stacking faults bounded by partial dislocations by transmission electron microscopy, TEM, in surface TiO_2 grains.[12] These defects most probably formed as a result of the thermal stresses generated due to thermal expansion mismatches during cooling. Cui et al. also confirmed the formation of Al_2TiO_5 above 1,400°C following the reaction:

$$TiO_2 + Al_2O_3 = Al_2TiO_5 \qquad (10)$$

This Al_2TiO_5 layer was correlated with the formation of cracks upon cooling. These cracks were ascribed to thermal expansion mismatches, and as importantly to the high anisotropy of thermal expansion of Al_2TiO_5. This compound has a CTE of $10.9 \times 10^{-6}\,K^{-1}$ along the *a*-axis, $20.5 \times 10^{-6}\,K^{-1}$ along *b* and $-2.7 \times 10^{-6}\,K^{-1}$ along *c*. The formation of Al_2TiO_5 should thus be avoided as much as possible.

Using TEM, Lin et al. explored the microstructures of Ti_3AlC_2 and Ti_2AlC samples after oxidation in air for 10 h at 1,200°C.[26] An enrichment of Ti in the Al_2O_3 grain boundaries and Ti-rich precipitates in the Al_2O_3 scales was identified. They also showed that Al depletion at the oxide/substrate interface was *minimal*, indirectly confirming that the diffusivity of Al in the carbides is quite fast at these temperatures. These results again emphasize the close similarities of the oxidation behavior observed in both Ti_3AlC_2 and Ti_2AlC.

Crack Healing. Before discussing the oxidation of Cr_2AlC, it is important to review a remarkable property of Ti_2AlC and Ti_3AlC_2, namely their crack healing ability.[27,28] Crack healing of Ti_3AlC_2 was investigated

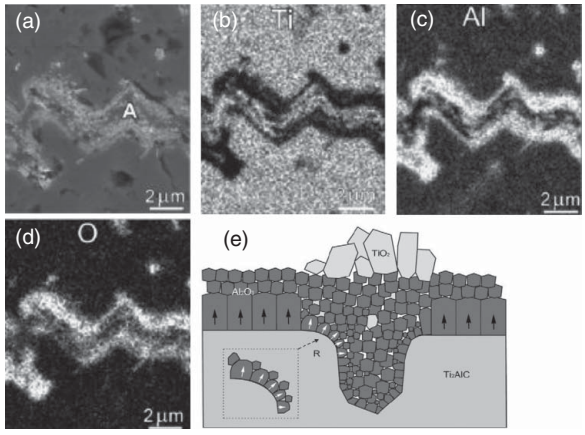

Figure 5. After oxidation at 1,100°C in air for 2 h, crack healing of Ti_3AlC_2 is seen via SEM micrographs (a) showing the formation of primarily α-Al_2O_3, as well as some rutile TiO_2; Energy dispersive X-ray spectroscopy element maps of the crack region show concentrations of (b) Ti, (c) Al and (d) O as the alumina forms in the crack. (e) A schematic of the process according to Ref. [27]

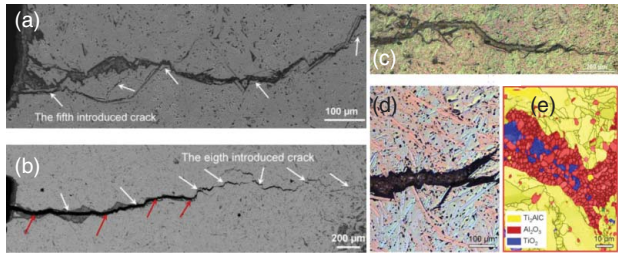

Figure 6. Images of fracture and crack healing in Ti_2AlC: (a) Crack path after four cycles of healing at 1,200°C for 2 h, and subsequent fracture. (b) Crack path after seven cycles of healing, and subsequent fracture. The red arrows indicate the location of remnant crack parts. (c) OM image of a crack fractured eight times before annealing in air at 1,200°C for 100 h showing the complete filling of the crack. (d) Enlarged OM image taken from (c). Two opposite fracture surfaces were covered by the same Al_2O_3 layer and the gap between the two surfaces was fully filled by a mixture of Al_2O_3 (black) and TiO_2 (white particles). (e) SEM image of the healed-damage zone obtained using electron backscatter diffraction.[29]

by oxidizing partially pre-cracked samples. A crack near a notch was introduced into the sample by tensile deformation. After oxidation at 1,100°C in air for 2 h, the crack was completely healed, with oxidation products consisting primarily of α-Al_2O_3, as well as some rutile TiO_2 (Figure 5(a)–(d)). A schematic of the process is shown in Figure 5(e). The indentation modulus and hardness of the crack-healed zone were slightly higher than those of the original Ti_3AlC_2 base material. The preferential oxidation of Al atoms in Ti_3AlC_2 grains on the crack surface resulted in the predominance of α-Al_2O_3 particles forming in a crack less than 1 μm wide.

In 2011, the same group [28] revisited the oxidation of Ti_2AlC and carefully examined the morphology of the various oxide layers that formed both on flat and curved surfaces or cracks. They found that after oxidation at 1,200°C for 16–100 h, the α-Al_2O_3 particles that formed on flat surfaces were small (≈1 μm), densely packed and columnar. Those that formed in the cracks or cavities, on the other hand, were more equiaxed and less densely packed. The rutile grains, however, exhibited a broad size distribution, ranging from sub-micrometer to 10 μm. The authors also confirmed the presence of small TiO_2 particles at the α-Al_2O_3 grain boundaries first reported by Lin et al.[26]

Even more recently, the same group [29] showed that Ti_2AlC was capable of repeatedly repairing damage events. When the authors introduced Knoop indentations on the tensile side of Ti_2AlC flexural bars, the flexural strength dropped from 211 ± 15 to 152 ± 20 MPa. Heating the indented bars, in air for two hours, resulted in an increase in the flexural strengths to 224 ± 50 MPa, a value that was slightly *higher* on average than the virgin samples, albeit with larger scatter. Even more impressively, after successively extending the same crack seven times and healing it between each fracture event, the fracture toughness dropped from ≈6.5 MPa$\sqrt{}$m, to about 3 MPa$\sqrt{}$m. It is important to note here that by the end of the seventh cracking iteration, the filled crack was of the order of 1 mm (Figure 6(a)). As in their previous work, Li et al. showed that the main healing mechanism at high temperature is the filling of the cracks by the formation of well adhering Al_2O_3 layers and some TiO_2 (Figure 6(b)–(e)). The authors write in their abstract: "Self-healing ceramics have been studied for over 40 years to obtain some performance recovery and to prevent material failure during service, but so far only materials with the capability of single healing event per damage site have been realized." They then proceed to show how Ti_2AlC is capable of multiple healing events.

Cr_2AlC. As noted above, the situation for Cr_2AlC is even more muddled, since most papers claim parabolic kinetics,[18–21,24] when as shown below they are far from parabolic. Figure 7(a) re-plots the results of Lin et al.[18] together with two power fits (solid lines), assuming cubic kinetics (dotted lines) and the parabolic rate constants reported by the authors (dashed lines). The power fits result in the following relationships at 1,200°C and 1,300°C, respectively

$$\Delta w(\mathrm{kg/m^2}) = 1.4 \times 10^{-4} \left(\frac{t}{t_o}\right)^{0.34}, \quad R^2 = 0.986, \tag{11}$$

$$\Delta w(\mathrm{kg/m^2}) = 8.8 \times 10^{-4} \left(\frac{t}{t_o}\right)^{0.25}, \quad R^2 = 0.977. \tag{12}$$

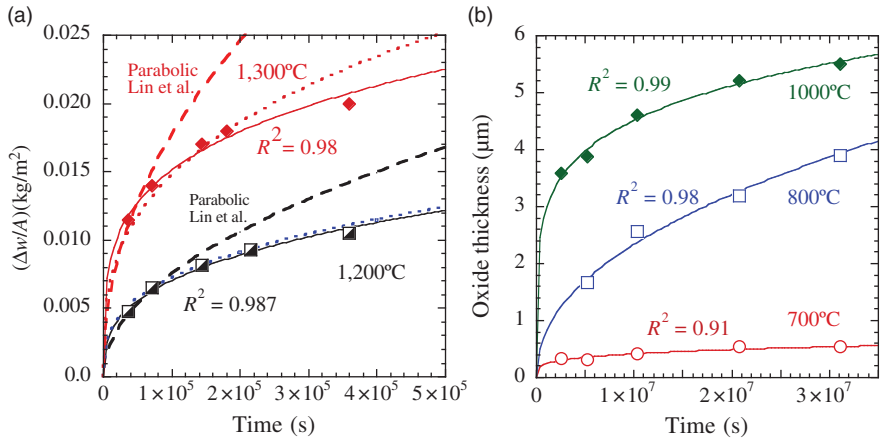

Figure 7. (a) Re-plots of the results of Lin et al.[18] together with two power fits (solid lines), assuming cubic kinetics (dotted lines) and the parabolic rate constants reported by Lin et al. (dashed lines) are shown. Cubic power fits result in time exponents of 0.34 and 0.25 for samples oxidized at 1,200°C and 1,300°C, respectively. (b) The same exercise in (a)—carried out on data by Lee et al.[23]—results in power fits shown by the solid lines with time exponent values of 0.24, 0.46 and 0.18 for samples oxidized at 700°C, 800°C and 1,000°C, respectively. With the possible exception of 800°C, the oxidation kinetics of Cr_2AlC are certainly not parabolic, and in most cases even better than cubic.

When the same exercise was carried out on some recent long-term oxidation (up to one year) results by Lee et al. [23] reproduced in Figure 7(b), the following relationships—shown by the solid lines in Figure 7(b)—for samples oxidized at 700°C, 800°C and 1,000°C, respectively, were obtained:

$$x(\mu m) = 0.009\left(\frac{t}{t_o}\right)^{0.24}, \quad R^2 = 0.91, \tag{13}$$

$$x(\mu m) = 0.001\left(\frac{t}{t_o}\right)^{0.46}, \quad R^2 = 0.98, \tag{14}$$

$$x(\mu m) = 0.24\left(\frac{t}{t_o}\right)^{0.18}, \quad R^2 = 0.99. \tag{15}$$

Taken *in toto* these results make it amply clear that with the possible exception of oxidation at 800°C, the oxidation kinetics of Cr_2AlC are certainly not parabolic, and for the most part, not even cubic. These results are noteworthy because they confirm that at 700°C, 1,000°C and 1,300°C, the oxidation kinetics are significantly *slower than cubic*. In other words, the time exponents are significantly less than 1/3. At 1,200°C they are close to cubic. The results at 800°C are anomalous, and reflect either enhanced oxidation kinetics at 800°C for reasons that are unclear and/or experimental uncertainty. If the first point at 800°C is ignored, the exponent value drops to about 0.38, which is probably more realistic. This comment notwithstanding, more work at 800°C is needed to better understand the nature of this possible anomaly.

In the final analysis, the oxidation kinetics of Cr_2AlC, for the most, part cannot be fit adequately with a simple model for the simple reason that the kinetics are initially relatively fast, but then slowly decrease with time to the point where the oxide layers almost stop getting thicker. The best example of this state of affairs can be found in the results shown in Figure 7(b). After 30 days of oxidation at 1,000°C, the oxide thickness was 3.5 μm; in the next 330 days, however, the oxide thickness increased by less than 2 μm.

Lastly, when all the results given in Table 1 are plotted on an Arhennian plot (Figure 8), it is clear that the absolute values of the cubic rate constants are comparable in the 1,100–1,200°C. However, at 507 ± 90 kJ/mol, the activation energy for the oxidation of Cr_2AlC is roughly double the 250 ± 30 kJ/mol for the Ti_2AlC and Ti_3AlC_2 compositions. Why the activation energies are so different is not clear at this time.

Note that the results listed in Table 1 all assumed cubic kinetics, when in some cases, as discussed above, the kinetics may not have been exactly cubic. The values listed in Table 1 are nevertheless useful because it is only by using them can the oxidation kinetics of the various materials be compared. However, for practical purposes where predictions of oxide thickness values at long times need to be made, the power law fits—with may be the omission of the first 10 or so hours—are to be used instead.

Implications of the Presence of Cr_7C_3 Layer after the Oxidation of Cr_2AlC Of more than 20 MAX phases whose oxidation response in air has been studied,[30–38] only one—Cr_2AlC—forms a carbide layer. This observation indirectly implies that for this compound C is *not* diffusing out as fast as the Al, which results in its accumulation at the substrate/oxide interface. This in turn implies that the alumina that forms on Cr_2AlC must be somewhat different from the one that forms on Ti_2AlC. Further evidence for the conclusion that

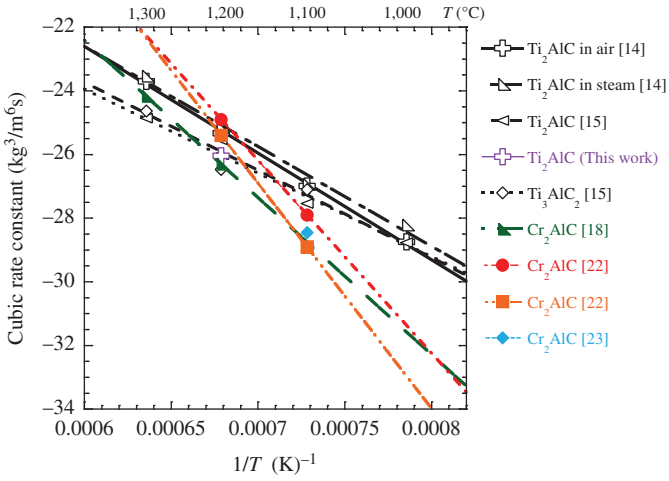

Figure 8. Arrhenian plot of cubic rate constants for Al_2O_3-forming MAX phases, Ti_2AlC, Ti_3AlC_2 and Cr_2AlC listed in Table 1.

the Al_2O_3 oxide layer that forms on Cr_2AlC is different than the one that forms on Ti_2AlC can be found in the over two orders of magnitude better corrosion resistance of Cr_2AlC to oxidation in the presence of Na_2SO_4, compared with Ti_2AlC or Ti_3AlC_2.[18] Lastly, a perusal of the results listed in Table 1 and shown in Figure 8 makes it clear that at all temperatures <1,200°C, Cr_2AlC has better oxidation resistance. Why this is the case is unclear at this time, but the dissolution of small amounts of Cr_2O_3 in the Al_2O_3 layer that forms when Cr_2AlC is oxidized [18,19,21,23,24] could play a role. Another factor may be the presence of small TiO_2 particles at the grain boundaries of the alumina that forms on Ti_2AlC.[6,8,10,13,14,26,29]

Note that the behavior of Cr_2AlC cannot be traced to the stability of Cr_7C_3 relative to TiC since the latter is significantly more stable. It is also unlikely that the anomalous behavior is associated with a low diffusivity of Al in Cr_2AlC since there is no reason to believe that the diffusivity of Al in Cr_2AlC is much different than it is in Ti_2AlC, which is fast enough to prevent any depletion of Al at the oxide/Ti_2AlC interface.

The presence of Cr_7C_3, however, is quite problematic for the simple reason that if for any reason the protective alumina layer is breached, the oxidation of the underlying carbide at high temperature would, more likely than not, be catastrophic (Figure 2(b)). When this is combined with the fact at 1,200°C, scale cracking and spalling is observed and at 1,300°C, the oxidation resistance deteriorates quickly as a function of cycling owing to the formation of voids and scale spallation,[20] it follows that despite its excellent oxidation resistance, it is unlikely that Cr_2AlC can be used at temperatures much higher than 1,100°C or even 1,000°C. Note the propensity for spallation can be traced to the relatively high CTE of this compound ($\approx 12.8 \times 10^{-6}$ K^{-1} [39]) relative to that of the protective alumina layer that forms.

Comparison to FeCrAl Alloys It is well documented that grain size coarsening leads to a decrease in oxide scale thickness growth rates in FeCrAl alloys, where inward oxygen diffusion dominates.[40–45] Naumenko et al. have shown a near cubic rate power law dependence by correlating oxide grain growth with the scale thickness, with a time dependence exponent ranging from 0.35 to 0.37 in FeCrAlY.[41] Liu et al. [42] developed a mathematical model to explain the dependence of scale thickness on oxide grain coarsening, which was seen to follow a $t^{1/3}$ dependence in the scale layer in FeAlCrY, in good agreement with previous work by Whittle et al.[43] Quadakkers et al. have criticized the use of parabolic rate calculations for determining the oxidation kinetics of α-Al_2O_3 in FeCrAl alloys, showing instead that they are better described by near cubic time dependencies with a power law fit.[40] Smeltzer et al. showed that the decrease in grain-boundary diffusion paths over time limits the inward diffusion of oxygen during oxidation.[46] As the area fraction of short circuit paths decreases, there is an overall decrease in oxide scale growth rates. Unsurprisingly, as discussed in the next section, the alumina layers formed herein are similar to those seen in other alumina forming materials (Figure 9).

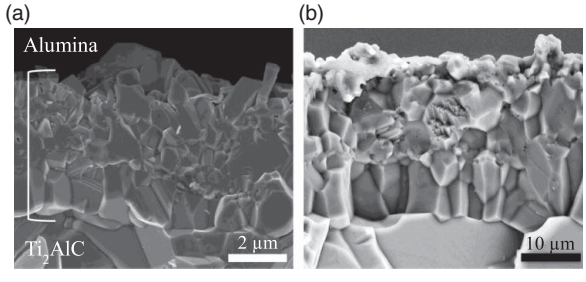

Figure 9. SEM micrographs of the fracture surface of Ti_2AlC after (a) 25 h and (b) 2,873 h at 1,200°C in air. Note clear increase in grain size with time.

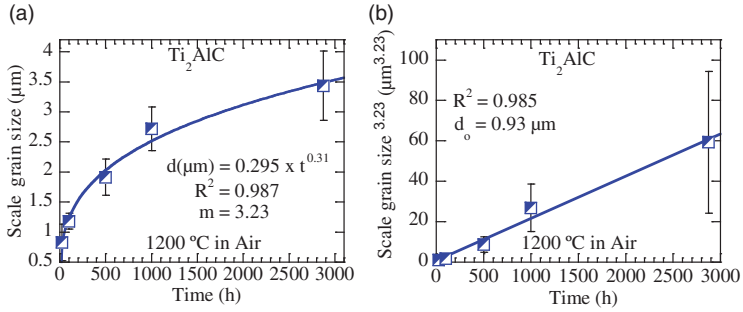

Figure 10. (a) Oxide scale grain coarsening kinetics plotted with a power law fit. (b) A least-squares fit of d^m vs. t results in a straight line, where the intercept is equal to d_o^m. At 0.93 μm, d_o is sufficiently small to assume that at long times it can be ignored in Equation (19).[42]

Modelling of the Oxidation Kinetics In general, the scale thickening rate can be written as [47]

$$\frac{dx}{dt} = D_{\text{eff}} \frac{\Delta\mu}{RT} \cdot \frac{1}{x}, \tag{16}$$

where D_{eff} is the effective diffusion coefficient, $\Delta\mu$ the oxygen potential difference between the scale/gas and scale/metal interfaces, and R and T are the universal gas constant and the temperature in degrees Kelvin, respectively.

If one assumes that the oxidation kinetics are controlled by grain-boundary diffusion of oxygen, then [48]:

$$D_{\text{eff}} = D_{\text{GB}} \frac{2\delta_{\text{GB}}}{r_G}, \tag{17}$$

where D_{GB} is the oxygen grain-boundary diffusion coefficient, δ_{GB} the grain-boundary width and r_{G} the oxide grain size.

In general, grain coarsening kinetics can be described by [49]

$$d^m = d_o^m + Kt, \tag{18}$$

where K is a constant, m is the grain growth exponent and d_o the initial grain size. Combining Equations (16)–(18), it can be shown that at longer times [42]:

$$x^2 \approx K' \left(\frac{t}{t_o}\right)^{(m-1)/m}, \tag{19}$$

where x is the scale thickness and K' is a constant (see [42]). It follows that if the assumptions made above are correct, then the following relationship applies:

$$n \approx \frac{(m-1)}{2m}. \tag{20}$$

To test this idea we measured the grain sizes of the alumina films that formed on the Ti_2AlC sample that was oxidized for almost 3,000 h. The results are shown in Figure 10(a). Based on the least-squares fit of the results, $m \approx 3.23$. According to Equation (20), $n \approx 0.345$, which, coincidentally or not, is in excellent agreement with the value of 0.36 derived from the results shown in Figure 3(b). Plotting $d^{3.23}$ vs. t (Figure 10(b)) results in a straight line fit, with intercept $d_o = 0.93$ μm, further validating the assumption—that d_o can be ignored at longer times—made in deriving Equation (19). Whether this agreement is fortuitous or not must await the results of further work at different temperatures and different alumina forming MAX phases.

Summary and Conclusions The oxidation resistances, in air, of the MAX phases, Ti_2AlC, Ti_3AlC_2 and Cr_2AlC are excellent because, in most cases, a dense, spall-resistant and protective Al_2O_3 layer forms. Of the three, and despite the fact that the oxidation kinetics of Cr_2AlC at temperatures <1,200°C are slower than those of Ti_2AlC (Figure 8), for practical applications Ti_2AlC is by far the most attractive for several reasons that include: (a) the higher concentration of Al as compared to Ti_3AlC_2, which is important because it increases the activity of Al at the substrate/oxide interface thus increasing the probability of the formation of the all-important alumina layer; (b) the excellent match between the thermal expansions of Ti_2AlC and alumina, which in turn minimizes thermal residual stresses and concomitant propensity of spallation; (c) lower density and (d) crack healing. Lastly, the fact that the raw materials for this MAX phase are some of the lowest costing of all MAX phases cannot be underestimated.

The formation of Cr_7C_3 upon the oxidation of Cr_2AlC is unique to this compound and implies that the alumina layer that forms is less pervious to C than the one that forms on Ti_2AlC, Ti_3AlC_2 and other MAX phases. The reason for this somewhat surprising result is unclear at this time.

At most temperatures, the oxidation kinetics are better described as cubic than parabolic. This comment notwithstanding, even cubic kinetics are an approximation. The best strategy to predict the time dependence of the alumina layer thickness is to fit the results to a power law fit. Lastly, by measuring the grain sizes of the alumina scale, we present evidence that the rate-limiting

step is diffusion of oxygen and/or aluminum ions down the alumina scale grain boundaries. The agreement with power law equations derived assuming grain-boundary diffusion is shown to be quite good. Further studies at different temperatures with other alumina forming MAX phases are indicated at this time to further confirm these conclusions.

Acknowledgements This research is supported by DOE's Office of Nuclear Energy University Program (DOE/NEUP).

References

[1] Barsoum MW. The $M_{n+1}AX_n$ phases and their properties. In: Riedel R, Chen I-W, editors. Ceramics science and technology. Weinheim: Wiley-VCH Verlag GmbH & Co. KGaA; 2010. p. 299–347.
[2] Barsoum M, El-Raghy T. Room-temperature ductile carbides. Metall Mater Trans A. 1999;30:363–369.
[3] Radovic M, Barsoum MW, El-Raghy T, Seidensticker J, Wiederhorn S. Tensile properties of Ti_3SiC_2 in the 25–1300°C temperature range. Acta Mater. 2000;48: 453–459.
[4] Radovic M, Barsoum MW, El-Raghy T, Wiederhorn SM, Luecke WE. Effect of temperature, strain rate and grain size on the mechanical response of Ti_3SiC_2 in tension. Acta Mater. 2002;50:1297–1306.
[5] Barsoum MW, Radovic M, Finkel P, El-Raghy T. Ti_3SiC_2 and ice. Appl Phys Lett. 2001;79:479–481.
[6] Barsoum M, Tzenov N, Procopio A, El-Raghy T, Ali M. Oxidation of $Ti_{n+1}AlX_n$ ($n = 1$–3 and $X =$ C, N): II. Experimental results. J Electrochem Soc. 2001;148:C551–C62.
[7] Barsoum M. Oxidation of $Ti_{n+1}AlX_n$ (n = 1-3 and X = C, N): I. model. J Electrochem Soc. 2001;148:C544–C50.
[8] Wang XH, Zhou YC. High-temperature oxidation behavior of Ti_2AlC in air. Oxid Met. 2003;59:303–320.
[9] Sundberg M, Malmqvist G, Magnusson A, El-Raghy T. Alumina forming high temperature silicides and carbides. Ceram Int. 2004;30:1899–1904.
[10] Byeon JW, Liu J, Hopkins M, Fischer W, Garimella N, Park K, Brady MP, Radovic M, El-Raghy T, Sohn YH. Microstructure and residual stress of alumina scale formed on Ti_2AlC at high temperature in air. Oxid Met. 2007;68:97–111.
[11] Wang XH, Zhou YC. Layered machinable and electrically conductive Ti_2AlC and Ti_3AlC_2 ceramics: a review. J Mater Sci Technol. 2010;26:385–416.
[12] Cui B, Jayaseelan DD, Lee WE. Microstructural evolution during high-temperature oxidation of Ti_2AlC ceramics. Acta Mater. 2011;59:4116–4125.
[13] Yang HJ, Pei YT, Rao JC, De Hosson JTM. Self-healing performance of Ti_2AlC ceramic. J Mater Chem. 2012;22:8304–8313.
[14] Basu S, Obando N, Gowdy A, Karaman I, Radovic M. Long-term oxidation of Ti_2AlC in air and water vapor at 1000–1300°C temperature range. J Electrochem Soc. 2012;159:C90–C6.
[15] Wang XH, Zhou YC. Oxidation behavior of Ti_3AlC_2 at 1000–1400°C in air. Corros Sci. 2003;45:891–907.
[16] Qian X, He XD, Li YB, Sun Y, Li H, Xu DL. Cyclic oxidation of Ti_3AlC_2 at 1000–1300°C in air. Corros Sci. 2011;53:290–295.
[17] Lee DB, Park SW. High-temperature oxidation of Ti_3AlC_2 between 1173 and 1473 K in air. Mater Sci Eng A. 2006;434:147–154.
[18] Lin ZJ, Li MS, Wang JY, Zhou YC. High-temperature oxidation and hot corrosion of Cr_2AlC. Acta Mater. 2007;55:6182–6191.
[19] Lee DB, Nguyen TD, Han JH, Park SW. Oxidation of Cr_2AlC at 1300°C in air. Corros Sci. 2007;49:3926–3934.
[20] Lee DB, Nguyen TD. Cyclic oxidation of Cr_2AlC between 1000 and 1300°C in air. J Alloys Compd. 2008;464: 434–439.
[21] Hajas DE, to Baben M, Hallstedt B, Iskandar R, Mayer J, Schneider JM. Oxidation of Cr_2AlC coatings in the temperature range of 1230 to 1410°C. Surf Coat Technol. 2011;206:591–598.
[22] Li S, Chen X, Zhou Y, Song G. Influence of grain size on high temperature oxidation behaviour of Cr_2AlC ceramics. Ceram Int. 2012:2715–2721.
[23] Lee DB, Nguyen TD, Park SW. Long-time oxidation of Cr_2AlC between 700 and 1,000°C in air. Oxid Met. 2012;77:275–287.
[24] Tian W, Wang P, Kan Y, Zhang G. Oxidation behavior of Cr_2AlC ceramics at 1100 and 1250°C. J Mater Sci. 2008;43:2785–2791.
[25] Pint BA. Experimental observations in support of the dynamic-segregation theory to explain the reactive-element effect. Oxid Met. 1996;45:1–37.
[26] Lin Z, Zhuo M, Zhou Y, Li M, Wang J. Microstructures and adhesion of the oxide scale formed on titanium aluminum carbide substrates. J Am Ceram Soc. 2006;89:2964–2966.
[27] Song GM, Pei YT, Sloof WG, Li SB, De Hosson JTM, van der Zwaag S. Oxidation-induced crack healing in Ti_3AlC_2 ceramics. Scr Mater. 2008;58:13–16.
[28] Yang HJ, Pei YT, Rao JC, De Hosson JTM, Li SB, Song GM. High temperature healing of Ti_2AlC: on the origin of inhomogeneous oxide scale. Scr Mater. 2011;65:135–138.
[29] Li S, Song G, Kwakernaak K, van der Zwaag S, Sloof WG. Multiple crack healing of a Ti_2AlC ceramic. J Eur Ceram Soc. 2012;32:1813–1820.
[30] Gupta S, Filimonov D, Barsoum MW. Isothermal oxidation of Ta_2AlC in air. J Am Ceram Soc. 2006;89: 2974–2976.
[31] Gupta S, A. G, D. F, W. BM. High-temperature oxidation of Ti_3GeC_2 and $Ti_3(Ge_{0.5}, Si_{0.5})C_2$ in air. Pennington, NJ: Electrochemical Society (ETATS-UNIS); 2006.
[32] Gupta S, Hoffman EN, Barsoum MW. Synthesis and oxidation of Ti_2InC, Zr_2InC, $(Ti_{0.5}, Zr_{0.5})_2InC$ and $(Ti_{0.5},Hf_{0.5})_2InC$ in air. J Alloys Compd. 2006;426: 168–175.
[33] Salama I, El-Raghy T, Barsoum MW. Oxidation of Nb_2AlC and $(Ti, Nb)_2AlC$ in air. J Electrochem Soc. 2003;150:C152–C8.
[34] Barsoum MW, Ho-Duc LH, Radovic M, El-Raghy T. Long time oxidation study of Ti_3SiC_2, Ti_3SiC_2/SiC, and Ti_3SiC_2/TiC composites in air. J Electrochem Soc. 2003;150:B166–B75.
[35] Chakraborty S, El-Raghy T, Barsoum MW. Oxidation of Hf_2SnC and Nb_2SnC in air in the 400–600°C temperature range. Oxid Met. 2003;59:83–96.
[36] Gupta S, Barsoum MW. Synthesis and oxidation of V_2AlC and $(Ti_{0.5}, V_{0.5})_2AlC$ in air. J Electrochem Soc. 2004;151:D24–D9.
[37] Amini S, McGhie AR, Barsoum MW. Isothermal oxidation of Ti_2SC in air. J Electrochem Soc. 2009;156: P101–P6.
[38] Barsoum MW, El-Raghy T, Ogbuji LUJT. Oxidation Of Ti_3SiC_2 in air. J Electrochem Soc. 1997;144:2508–2516.

[39] Scabarozi TH, Amini S, Leaffer O, Ganguly A, Gupta S, Tambussi W, Clipper S, Spanier JE, Barsoum MW, Heffiger JD, Lofland SE. Thermal expansion of select $M_{(n+1)}AX_n$ (M = early transition metal, A = A group element, X = C or N) phases measured by high temperature x-ray diffraction and dilatometry. J Appl Phys. 2009;105:013543–013548.
[40] Quadakkers WJ, Naumenko D, Wessel E, Kochubey V, Singheiser L. Growth rates of alumina scales on Fe–Cr–Al alloys. Oxid Met. 2004;61:17–37.
[41] Naumenko D, Gleeson B, Wessel E, Singheiser L, Quadakkers WJ. Correlation between the microstructure, growth mechanism, and growth kinetics of alumina scales on a FeCrAlY alloy. Metall Mater Trans A. 2007;38: 2974–2983.
[42] Liu Z, Gao W, He Y. Modeling of oxidation kinetics of Y-doped Fe–Cr–Al alloys. Oxid Met. 2000;53: 341–350.
[43] Whittle DP, Stringer J. Improvements in high temperature oxidation resistance by additions of reactive elements or oxide dispersions. Philos Trans R Soc Lond Ser A Math Phys Sci. 1980;295:309–329.
[44] Quadakkers WJ. Growth mechanisms of oxide scales on ODS alloys in the temperature range 1000–1100°C. Mater Corros. 1990;41:659–668.
[45] Young DJ, Naumenko D, Niewolak L, Wessel E, Singheiser L, Quadakkers WJ. Oxidation kinetics of Y-doped FeCrAl-alloys in low and high pO2 gases. Mater Corros. 2010;61:838–844.
[46] Smeltzer WW, Haering RR, Kirkaldy JS. Oxidation of metals by short circuit and lattice diffusion of oxygen. Acta Metall. 1961;9:880–885.
[47] Birks N, Meier GH, Pettit FS. Introduction to the high temperature oxidation of metals. Cambridge: Cambridge University Press; 2006.
[48] Atkinson A. Transport processes during the growth of oxide films at elevated temperature. Rev Mod Phys. 1985;57:437–470.
[49] Kingery WD. Introduction to ceramics. 4th ed. New York: Wiley; 1960.